

Framatome ANP, Inc.
An AREVA and Siemens company

BAW-2241NP
Revision 2
Appendix G
Revision 1

Fluence and Uncertainty Methodologies

G.1 Introduction

The purpose of this appendix is to update the uncertainties that are associated with boiling water reactor (BWR) fluence calculations. In previous revisions to this topical, Framatome ANP showed that its fluence uncertainty methodologies applied to all pressurized water reactors (PWR). The benchmarks in this revision show that the Framatome ANP (FANP) methodology that was accepted for PWR licensing applications in Revision 1 can be appropriately modified for BWRs. The benchmarks of the BWR methodology described in this appendix constitute Revision 2 to BAW-2241P.

Before developing this appendix, Framatome ANP held discussions with the NRC concerning the required content for its acceptance. It was agreed that the basic methodology for the fluence calculations, dosimetry measurements, and uncertainty evaluations would be the same for PWRs and BWRs. However, a set of BWR benchmarks was necessary to show consistency between the uncertainty in the BWR fluence methodology and uncertainties and the FANP database.

The basis of the theoretical methodology for calculating the fluence in a BWR is the same as that for a PWR. The DORT^{G1} computer code is used in the same manner for both, and both use the BUGLE-93⁷ cross section library. The source term for PWRs and BWRs is developed from core-follow data that matches the in-core operational measurements of the three dimensional power. Since the theoretical methodology for BWRs is the same as that for PWRs, the uncertainty methodology would also be the same. However, the complexity associated with varying water densities in the axial segments of BWR fuel assemblies introduces an additional uncertainty into the analytical

PROPRIETARY

modeling. Thus, the BWR uncertainties have been validated using the aforementioned methods. The estimated value of the uncertainty for BWR and PWR results is the same.

This appendix presents the calculational methodology that has been updated for BWR fluence evaluations. It also presents the BWR benchmarks and calculational uncertainty.

G.2 Background

As explained in Revision 1 of this topical, the Framatome ANP dosimetry database has measurements (M) with certified uncertainties from reference field validation by the National Institute of Standards and Technology. Thus, the FANP benchmarks include a certified uncertainty for the calculated (C) results as well as the benchmark C/M uncertainties.

The NRC noted that confirmatory benchmarks are necessary to have a valid estimate of BWR uncertainties. The NRC indicated that sufficient benchmarks would be (1) the PCA results,^{G4} (2) the comparison to the NRC BWR benchmark problem in NUREG/CR-6115,^{G5} and (3) a capsule comparison from an operating plant.^{G6}

To confirm that the BWR uncertainties estimated in this appendix have the appropriate level of confidence, the results from the benchmark comparisons noted above must be consistent with the existing FANP database. For the PCA, the comparison needs to review the consistency with the BWR geometry. For the NRC BWR benchmark problem, the deviations between the Brookhaven National Laboratory (BNL) and FANP results must be consistent with the deviations that were associated with the PCA results. Finally, for the operating plant capsule comparison, the deviations must be consistent with the FANP database.

The accuracy of the BWR fluence calculations is identical to the previously reported results for PWRs. The BWR benchmark comparisons provide confidence that the uncertainties are within the population of the FANP benchmark database.

G.3 Extension of Fluence Methods

Revision 1 of the topical report presents two methodologies, one for determining the fluence and the other for estimating the uncertainty in the methodology for determining the fluence.

There are two major parts of Framatome ANP's methodology for determining the fluence. The first part is the evaluation of dosimetry measurements. The second is the calculation of the fluence throughout the reactor internal structures, vessel, and reactor shield-support structure within the beltline region.

The theoretical and experimental methods used to determine the calculated and measured results for the fluence and dosimetry activities are not dependent on the reactor design. Thus, the theoretical and experimental methods (DORT, BUGLE-93, etc.) for BWRs are the same as those for PWRs. While the approximations used to obtain solutions to the theoretical methods for PWRs need to be extended when applied to BWRs, the measurement process requires no extension of the techniques or procedures. Consequently, the experimental methodology is not discussed in this section. The BWR experimental methods are the same as those discussed in Section 5 of this topical report. This section addresses the BWR calculational models and procedures used in the solution of the theoretical methods.

PROPRIETARY

G.3.1 Solution of BWR Fluence Methods

The fluence methodology presented in this report describes theoretical methods, with procedural and modeling approximations that provide accurate and reliable predictions of the greater than 0.1 MeV fluence values. These methods were originally developed for PWRs but they are generic to any water-moderated reactor. Consequently, the PWR calculational models and procedures are utilized as the basis for calculating the fluence throughout the internal components and vessel of BWRs. While the PWR approximations are generic to any water moderated reactor, there are three areas where the approximations must be expanded to provide accurate and reliable predictions of the greater than 0.1 MeV fluence values for BWRs. The following discussion explains the development process that led to the identification of the three areas. The discussion continues by explaining the development of the expanded models and procedures to ensure the same accuracy in the results as previously shown by the benchmark database.

In 2001, Framatome ANP formed a joint venture with Siemens that possessed BWR technology. The joint venture provided valuable expertise for applying PWR fluence methods to BWR designs. Three areas that were found to require an extension of the PWR models and procedures to analyze BWR vessel fluence values were: (1) the transport of neutrons from the core through the internal structures associated with the jet pumps, (2) the integrated core leakage function from the fuel, and (3) the three dimensional synthesis of the core leakage function.

G.3.2 Neutron Transport Through Jet Pumps

Neutron transport from the core region through the internals and other reactor structures is envisioned as being divided into two parts for the purpose of this discussion. The first part involves the leakage of neutrons from the core. The second involves the transport of the neutrons through the internal components and vessel to the concrete shield and support structure. The Framatome ANP models and procedures used to obtain a solution to the transport process in the second part are equally applicable in PWRs and BWRs. However, if BWR dosimetry is located within the radiation shadow area of the jet pumps, the modeling of the pump structures must include the same type of procedures for [] accuracy as those used in PWRs []

Figure 3-2 represents a schematic of the radial plane of a PWR. To model this geometry, a cylindrical coordinate system (r, θ) is used. However, there is a problem []

]

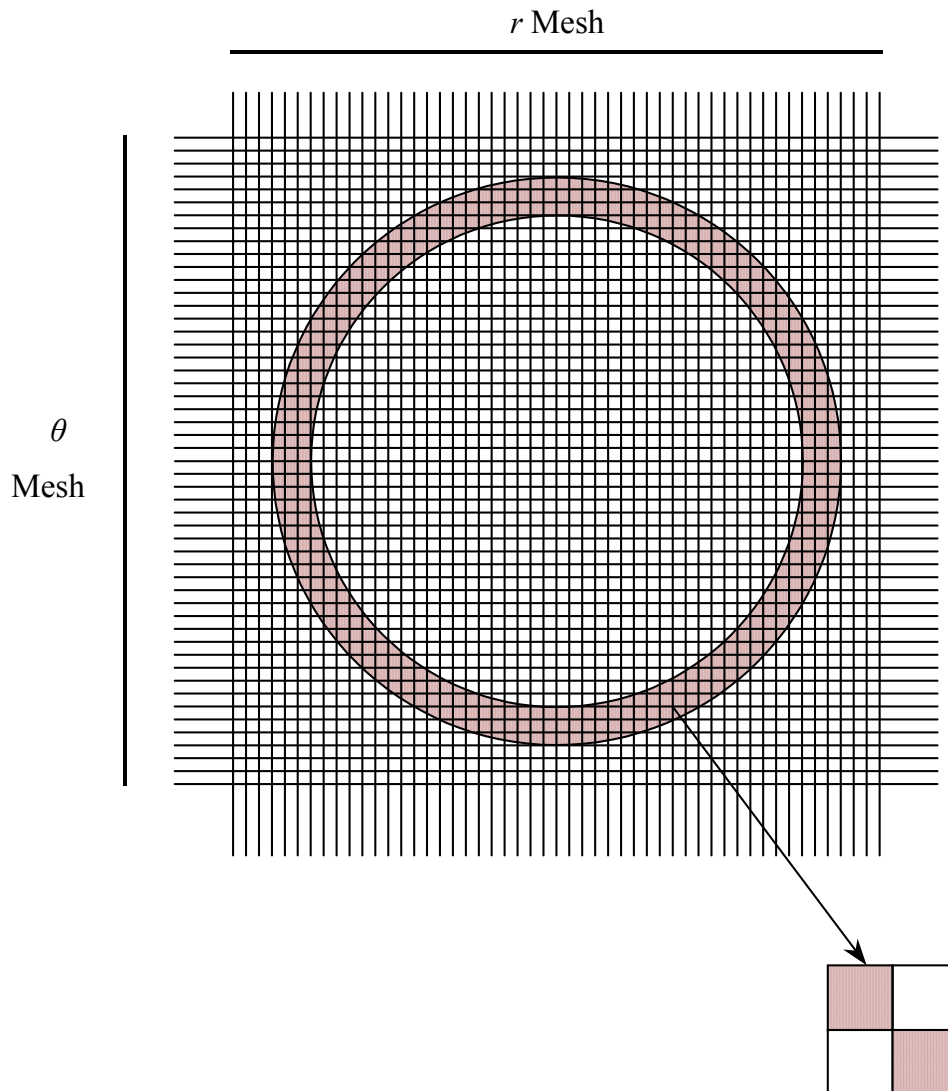
Figure G-1 represents a schematic of a cylindrical section of a jet pump component in the radial plane. The vessel flux is shielded from the neutrons leaking from the core by the internal structures, such as the jet pumps. Therefore, the maximum vessel flux does not occur in the shadow behind the jet pump structures. Therefore, the evaluation of the maximum flux does not need an accurate pump model. However, the evaluation of the dosimetry in the shadowed area behind the jet pump structures is affected by the pump modeling. [

] The following discussion reviews the models and procedures used to attain the needed accuracy in the flux calculations.

Reviewing Figure G-1, the jet pump structure is schematically shown in the radial plane as the “shaded” tubular region. The coordinates, noted by the square crosshatch of grid lines, are cylindrical.

PROPRIETARY

Figure G-1
Schematic of r, θ Modeling
For Jet Pump Tubular Structure



PROPRIETARY

The abscissa (horizontal line) is noted as the radial (r) coordinate, and the ordinate (vertical line) is noted as the angular (θ) coordinate. [

]

The extension of the Framatome ANP models and procedures to BWR jet pumps provides a means of accurately evaluating dosimetry reactions near the pumps. [

]

G.3.3 Core Leakage Function

An important consideration in the flux solution for vessel fluence evaluations is the leakage of neutrons from the core. The Framatome ANP methods are based on the solution of the three dimensional (\mathbf{r}) fission rates integrated over the energy (E) and angular variables ($\mathbf{\Omega}$) of the velocity groups (g), and time (t). The accuracy of the process begins with the core-follow simulation of the measured fission rates for power production. The core-follow results match the measurements within the uncertainty criteria for the magnitude of the power and distribution.

The measurements of core operation are taken at periodic intervals. The core-follow simulation of the operation utilizes the measured data from each period to follow the power production. Given the close relationship between the calculated three dimensional power distribution and the comparable measurements of axial segments for each assembly, the core-follow time-steps provide a numerical means of integrating the fission rates over the operational cycles. The average time-weighted source parameters are those given in Equations 3.1 and 3.2. As shown by the equations, the neutron source terms are represented by three dimensional (\mathbf{r}) values for each fuel rod and axial rod segment. These sources are processed for the cylindrical coordinate system used in the DORT modeling.

Since the discrete source eigenfunctions represent a solution to the three dimensional neutron transport equation, these source eigenfunctions may be returned to a three dimensional neutron transport model to serve as a “fixed” source term. The neutron transport theory expression with a “fixed” source eigenfunction $\{S(\mathbf{r}, E, \mathbf{\Omega})\}$ is represented by Equation G.4.

$$\boldsymbol{\Omega} \cdot \nabla \phi(\mathbf{r}, E, \boldsymbol{\Omega}) + \Sigma_T(\mathbf{r}, E) \phi(\mathbf{r}, E, \boldsymbol{\Omega}) = S(\mathbf{r}, E, \boldsymbol{\Omega}) \quad (\text{G.4})$$

The average time-weighted collision density parameters $\{\Sigma_T(\mathbf{r}, E) \phi(\mathbf{r}, E, \boldsymbol{\Omega})\}$ from the three dimensional core-follow calculations are evaluated using the same procedures as those used for the source parameters. Assuming that there is no average time-weighted effect on the leakage function $\{\boldsymbol{\Omega} \cdot \nabla \phi(\mathbf{r}, E, \boldsymbol{\Omega})\}$, the collision density parameters and source parameters in Equation G.4 produce the same flux values as those from the average time-weighted core-follow calculations.

[

]

Using the models and procedures discussed in Section 3 of this topical to compute BWR leakage rates from the core periphery indicates that the approximations in the modeling and procedures must be updated. The average time-weighted “fixed” source

PROPRIETARY

eigenfunctions and collision density parameters do not produce accurate peripheral flux values. To understand the failure in the approximations, the solution of Equation G.4 needs to be reviewed. DORT provides a general numerical solution of Equation G.4, but it is not useful to evaluate the relationship between the leakage rate, collision density, and source density. [

]

The neutrons crossing the boundary between \mathbf{r}' and \mathbf{r} represent the leakage of source neutrons from \mathbf{r}' . If we consider a fuel region defined by an array of \mathbf{r}' mesh positions, the leakage from the \mathbf{r}' region is evaluated by integrating the current density at the surface of the fuel, the boundary of \mathbf{r}' . The leakage of the greater than 0.1 MeV flux from the surface of the fuel region is expressed by the Equation G.6 integrals over energy (E), angle ($\boldsymbol{\Omega}$), and the surface area (A) perpendicular (\perp) to a unit of the vector “ $\mathbf{r}'_{\perp A}$ ” in the direction of the neutron current from the region.

PROPRIETARY

$$Leakage(\bar{\mathbf{r}}, \bar{E}, \bar{\boldsymbol{\Omega}}) = \int_A \int_E \int_{\boldsymbol{\Omega}} \boldsymbol{\Omega} \cdot \left(\frac{\mathbf{r}'_{\perp A}}{|\mathbf{r}'|} \right) \phi(\mathbf{r}', E, \boldsymbol{\Omega}) dA dE d\boldsymbol{\Omega} \quad (G.6)$$

[]

Substituting the equivalent Equation G.5 solution into the integral part of Equation G.6 gives the leakage [] with energies greater than 0.1 MeV and an exponential integral function ($f_{leakage}$). Since (a) the current density is determined by the angular integral of the vector flux density $\{\boldsymbol{\Omega} \phi(\mathbf{r}, E, \boldsymbol{\Omega})\}$, and (b) the source density produces the flux from the leakage, and scattering reaction $\{\Sigma_s(\mathbf{r}', E) \phi(\mathbf{r}', E, \boldsymbol{\Omega})\}$ rate densities, []

]

PROPRIETARY

During any one cycle of operation and for many successive reload cycles, the water density in an axial segment of a PWR fuel assembly is essentially constant. Therefore, the collision rate $\{\Sigma_T(\mathbf{r}', g) \phi(\mathbf{r}, g, \Omega_n)\}$ in the fuel region is directly proportional to the source $\{S(\mathbf{r}', g, \Omega_n)\}$ [

] These approximations in the PWR models and procedures produce accurate flux results within the core region of the peripheral fuel assemblies, and for dosimetry reactions. However, in a BWR model, the core and dosimetry calculational accuracy is insufficient. The problem is that the water concentration (N^{Water}) in an axial segment of a fuel assembly varies during a cycle, and may vary from cycle to cycle for the assemblies located in the same position on the periphery of the core. Consequently, the total cross section $\{\Sigma_T(\mathbf{r}', g)\}$ varies with time during the operation of the various cycles.

[

PROPRIETARY

] Equation G.7 gives the expression for extending the core leakage model
[
] (G.7)

In Equation G.7, the symbol “ $f_{leakage}^{-1}$ ” represents the inverse operation of the
Equation G.6 leakage function, $f_{leakage}$. [

]

Using the models and procedures discussed in Section 3 of this topical report to compute BWR leakage rates from the core periphery indicates that the approximations in the models and procedures are insufficient. [

]

G.3.4 Three Dimensional Synthesis

The fluence calculational methodology discussed in the previous sections of this topical report begins with “exact” three dimensional ($\mathbf{r}; x, y, z$) core-follow analyses (no synthesis approximation) for the core region. Reviewing the results from any PWR model shows that all cores that operate without control rods or non-uniform poison shields have only one unique axial (z) power shape. Moreover, those cores that operate with axial power shaping rods (B&W plants) can be modeled using only one unique axial

PROPRIETARY

power shape for fluence (rate) calculations. Thus, collapsing the “exact” three dimensional model to two dimensional models (x, y) or (r, θ) is a straightforward integral process. It is also straightforward to integrate the r, θ model over the θ direction and incorporate the z - source distribution when developing the r, z model.

When the peripheral fuel of a PWR core has axially segmented fuel assembly components to shield a critical weld location, multichannel - planar models, with piecewise continuous axial shape functions, are necessary for calculating the three dimensional effects. However, the models and procedures continue to be clear-cut. The number of discrete axial channels is generally no greater than four.

BWR fluence analyses, like the PWR analyses, begin with “exact” three dimensional core-follow models in the core region. Reviewing the results from BWR analyses shows that there are many unique axial (z) power shapes associated with normal operation. Not only does the inserted position of the control rods contribute to various distinctive axial shapes, but the degree of boiling also creates unique axial power shapes.

The degree of boiling is a function of the axially integrated power in the channel of each assembly. Each assembly in the core with a different “assembly” power will have a different axial power shape. Due to the many unique “assembly” powers and axial power shapes in the BWR core, collapsing the “exact” three dimensional model to two dimensional models for fluence analysis is more complex than Section 3.3 discussed previously. In addition, the coupling of the boiling water density and the axial power shape, along with the control rod position and the axial power shape does not provide an accurate means of axially integrating the water density and control rod effects for a r, θ model. [

]

Due to the complexity of collapsing the “exact” three dimensional model of the core to two dimensional models for three dimensional synthesis analysis of the vessel fluence, the best method for calculating the three dimensional flux would appear to be an “exact” three dimensional model (e.g. TORT). However, the accuracy of three dimensional models is very poor. The problem fundamentally is not the calculational methods. Instead, the physical limitations associated with the computer are the governing factor. For each of the sixty seven BUGLE energy groups, and each of the one million mesh points used in the three dimensional modeling, there are on the order of one hundred directional flux values. This results over six billion values for the flux solution that must be iteratively evaluated. Therefore, the three dimensional synthesis model has been extended for BWR analyses.

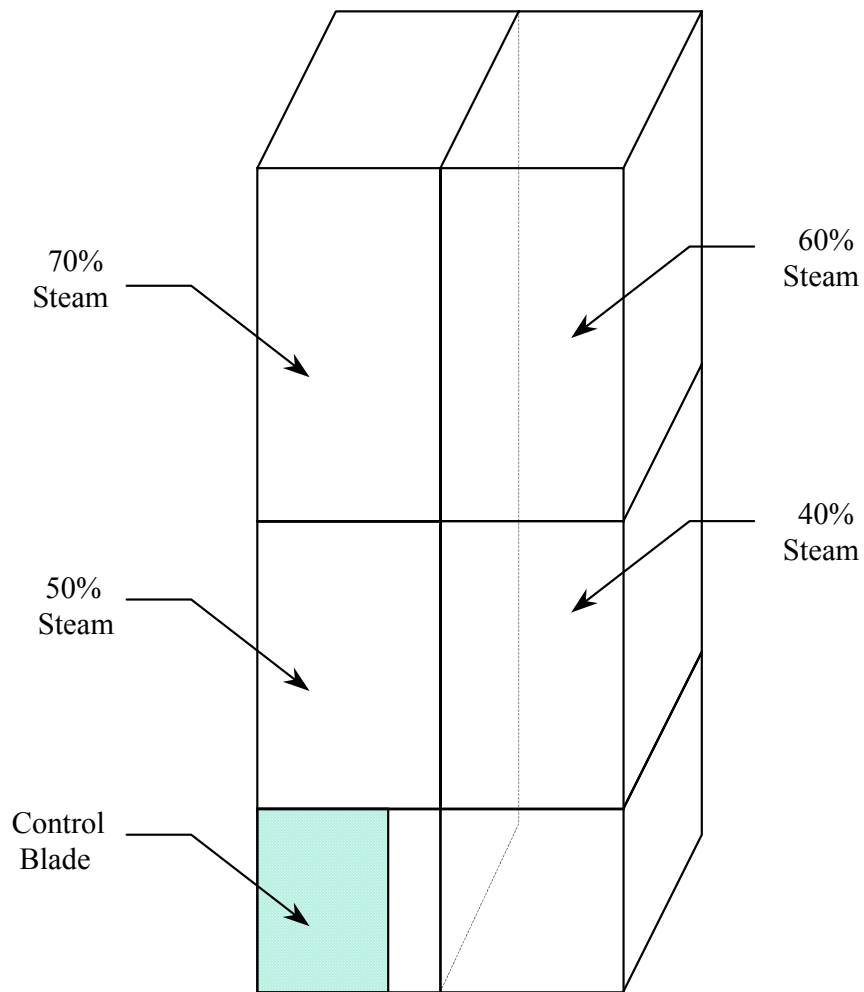
[

]

The axial spacing of the planar regions is developed from the “exact” three dimensional core-follow model. The core-follow model results are used to identify the axial shape functions that best represent the effects of the control rod positions and the degree of channel boiling. The axial spacing of the planar regions is not uniform since inflections in the shape functions do not generally occur in equal increments.

PROPRIETARY

Figure G-2
Schematic of Three Dimensional Synthesis
For BWR Fuel Assemblies



PROPRIETARY

Figure G-2 provides a schematic of two boiling water fuel assemblies. The purpose of the schematic is to help explain the extension of the synthesis methods. The schematic is not as detailed as the synthesis model. Instead, it represents three unequally spaced planar regions for the axial mesh spacing rather than seven or more. Each synthesis and schematic planar region represents a combination of x, y or r, θ planar regions from the core-follow model. Viewed from the top of the figure, looking down, the x, y assembly pitch of the radial plane of the core region would be obvious. The combination of axial segments from two or more planar regions in the core-follow model would give one of the assembly segments that are shown in Figure G-2.

$$S^{3D}(x, y, \overline{\delta z}, \overline{E}, \overline{\Omega}) = \frac{\int_{\delta z} S^{3D}(x, y, z, \overline{E}, \overline{\Omega}) dz}{\int_{\delta z} dz} \quad (G.8)$$

Equation G.8 expresses the integration of the three dimensional (3D) source function (S) for each planar region segment of a fuel rod modeled in the synthesis calculation. In Figure G-2, the Equation G.8 3D source function is schematically associated with the axial segment of one assembly. To develop the source function for a two dimensional “ $R\theta$ ” synthesis calculation, a z -dependent multichannel source function (S_C^Z) is used as shown by Equation G.9.

$$[\quad \quad \quad](G.9)$$

PROPRIETARY

The x, y or r, θ planar regions in the “ $R\theta$ ” synthesis calculation not only include the Equation G.9 source functions in each axial segment, but the functional weighting of the collision reactions is also included. As discussed above, the core-follow time-steps provide a numerical means of integrating the source and collision parameters over the operational periods of interest for the fluence evaluations. [

](G.10)

[

]

PROPRIETARY

To summarize, the Framatome ANP synthesis models and procedures described in Section 3.3 of this revision are appropriate for BWR calculations. However, the multichannel - planar models used previously for PWRs has been expanded for BWRs. The reason for the modeling-procedure extension is the multiple time-dependent, non-separable, axial power shapes, which result from control rod insertion and channel boiling during operation. The shapes from each core-follow time-step are integrated into average time-weighted axial shapes for each assembly. These time-weighted, average assembly shapes provide the basis for the BWR multichannel modeling. The extension of Framatome ANP's models and procedures for BWR synthesis calculations involves more channels than previously evaluated and thereby more calculations to obtain the integrated coupling of the " $R\theta$ " planes with piecewise axial shape functions.

The extended models and procedures for synthesis calculations of BWRs are validated in the same manner as the core leakage function and the transport of neutrons through the jet pumps. The DORT results must agree with the results from calculations that have a defined degree of accuracy, such as those from the core-follow model. If the approximations used in the DORT modeling and analysis procedures are valid, the results from the DORT synthesis will be accurate in comparison to the reference three dimensional (core-follow) calculations. [

]

The methodology presented in this appendix includes a more accurate treatment of (1) the transport of neutrons from the core through the internal structures associated with the jet

PROPRIETARY

pumps, (2) the integrated core leakage function from the fuel, and (3) the three dimensional synthesis of the core flux function. With the more accurate treatment, the methodology presented in this appendix is appropriate for calculating the flux throughout the internal structures and vessel of BWRs.

G.4 Uncertainty Update

This topical report presents two methodologies, one for determining the fluence and the other for estimating the uncertainty in the methodology for determining the fluence. The fluence and uncertainty methodologies are fundamentally theoretical methods that include procedural and modeling approximations. The theoretical methods are generic to all light water reactors (LWRs). While the models and procedures discussed in the original revision BAW-2241P-A submittal are generic, the results in Appendix A, “FANP’s Dosimetry Database” are weighted with more B&W plants. The statistical evaluation of the models and procedures was expanded in Appendix E, Revision 1 of BAW-2241P-A, to weight all PWR plants equally. This section extends the discussion of the uncertainty evaluation to all LWR plants.

Uncertainties are evaluated for the (1) measurements, (2) calculations, and (3) benchmark comparisons of the calculations to the measurements. Two types of deviations, systematic and random, characterize these uncertainties. The systematic deviations are caused by inaccurate results with one or more unique biases producing the errors. The random deviations have no specific cause. However, the standard deviation from a “normal” distribution function that is estimated using mathematical statistics represents the precision of the overall random uncertainty. The mathematical statistics processing of the distribution of random deviations provides a level of confidence in the precision of

PROPRIETARY

the results. The level of confidence in the fluence uncertainty needs to be consistent with the level of confidence in the embrittlement uncertainty.

G.4.1 Measurement Uncertainties

One essential part of the uncertainty methodology is that all uncertainties must be defined in terms of reference standards that are known to be “true” values. As explained in the regulatory guide for determining the vessel fluence,^{G3} the measured results are not “true” values unless they have been validated by a National Institute of Standards and Technology (NIST) reference field. The NIST reference field validation is more than the usual calibration standards for the experimental equipment. It is the validation of the measured dosimetry results by a NIST team. The NIST team independently performs the measurements and compares their results to those of the B&W laboratory. Moreover, the NIST team reviews each part of the experimental process. By reviewing each part, they determine if any small biases exist and whether any biases essentially cancelled each other. As explained in Framatome ANP’s “Standard and Reference Field Validation” document,^{E3} NIST certified the laboratory that FANP uses to have no statistically significant biases. Thus, the mean value of the measured results is accurate and only varies randomly about the “true” value. NIST also confirmed that the laboratory’s estimate of the standard deviation in the random uncertainties provided the appropriate level of confidence in the variation of the mean measurement about the “true” value.

The dosimeters associated with BWR specimen capsules are of the same type and form as those validated by NIST for the B&W laboratory measurements. Consequently, the Framatome ANP evaluation of BWR dosimetry measurements is valid.

PROPRIETARY

The Framatome ANP dosimetry measurements have no statistically identifiable bias and have a standard deviation that is not greater than 7.0%.

$$\textit{Mean Measurement Uncertainty} \leq 7.0\%$$

(G.11)

G.4.2 **Calculational Uncertainties**

The uncertainties in the calculational methodology are determined from two evaluations, a computational sensitivity of the parameters affecting the calculations, and a benchmark of the calculated dosimetry results to the measurements. The parameters affecting the solution of Equation G.4 are evaluated using a set of sensitivity calculations of the neutron source, geometry, material composition, and modeling. The statistical combination of the fluence rate deviations from the sensitivity evaluations provides an estimate of the standard deviation in the dosimetry reactions and greater than 0.1 MeV vessel fluence values. The DORT results from Equation G.4 are compared to the Framatome ANP dosimetry database to evaluate biases statistically, [

]

The benchmark of the dosimetry database provides the means of evaluating biases in the calculational methodology [

] The following discusses

(1) the PCA benchmark results, (2) the FANP comparison to the NRC BWR benchmark problem in NUREG/CR-6115, and (3) the comparison of FANP capsule calculations for Browns Ferry Unit 2.

G.4.2.1 Pool Critical Assembly Benchmark

The Pool Critical Assembly (PCA) is a test reactor located at the Oak Ridge National Laboratory (ORNL). Between September the third of 1978 and January the fourteenth of 1981, the PCA was setup to simulate two different reactors. The reactors are designated by the respective water region widths of the reflector and downcomer. Reactor operation

PROPRIETARY

activated the dosimetry in seven locations along the axis as shown in Figures 1.1.2 and 1.1.3 of Reference G4. The importance of the measurements was to serve as a “blind test.” Each participant making fluence predictions for the utility industry would submit their results prior to knowing the results of the measurements. ORNL and the NRC judged the accuracy and precision of the participants. Framatome ANP (participant “Y”) had the most accurate results.

As explained in Reference G4, the dosimetry measurements for locations “A1” and “A3M” are not as accurate as those for locations “A4” through “A6”. Consequently, the NRC has focused on these later three locations for the dosimetry results.

The key to these locations for the BWR benchmark is that, a calculational methodology that is accurate, and shows no correlation of the random deviations, will remain accurate, independent of the steel and water configurations of the internal and vessel structures. Therefore, when the FANP calculations of the dosimetry in locations “A4” through “A6” are compared to the measurements for the reactor with an “8” centimeter reflector and a “7” centimeter downcomer (8/7), there should be no obvious trend in the ratio of calculations to measurements, C/M . Moreover, when the calculations of the “A4” through “A6” dosimetry are compared to the measurements for the reactor with a “12” centimeter reflector and a “13” centimeter downcomer (12/13), there should be no

PROPRIETARY

obvious trend in the ratio of calculations to measurements either for the dosimetry locations or the two different reactor internal configurations. The following excerpts the FANP results.

| 8/7 Configuration: C/M Comparison | | | |
|---|-----------------|-----------|-----------|
| | Location | | |
| Dosimetry | A4 | A5 | A6 |
| $^{237}\text{Np}(n,f)$ | 0.92 | 0.92 | 0.87 |
| $^{58}\text{Ni}(n,p)$ | 0.92 | 0.88 | 0.88 |
| $^{27}\text{Al}(n,\alpha)$ | 0.91 | 0.89 | 0.90 |
| $^{238}\text{U}(n,f)$ | 0.85 | 0.83 | 0.79 |
| 12/13 Configuration: C/M Comparison | | | |
| $^{237}\text{Np}(n,f)$ | 0.98 | 0.98 | 0.96 |
| $^{58}\text{Ni}(n,p)$ | 0.94 | 0.86 | 0.94 |
| $^{27}\text{Al}(n,\alpha)$ | 0.96 | 0.93 | 0.94 |
| $^{238}\text{U}(n,f)$ | 0.90 | 0.87 | 0.85 |

The standard deviation for the dosimetry measurements varies. It was estimated that the ^{238}U may be as high as 15% due to ^{235}U impurities and photofissions, the ^{237}Np may be about 10%, and the ^{27}Al and ^{58}Ni may be as low as 6%. In addition to the dosimetry measurement uncertainties, there is an uncertainty of 4% associated with the PCA absolute power. Using the FANP database, the calculational uncertainty is [

] As discussed in Reference G4, the overall ratio of calculational results to measurements for all participants was somewhat less than 1.0. This indicates that there is a bias in the PCA measured data. Independent of a possible measurement bias, the C/M comparisons for the dosimetry locations in both the 8/7 and 12/13 configurations indicate that the FANP calculations have no bias as a function of spatial location or as a function of steel – water configurations. Moreover, the combined

PROPRIETARY

calculational and measurement standard deviation (σ) for the C/M comparisons ($\overline{\sigma_{C/M}}$) is 17.0% for the ^{238}U dosimeters, 12.8% for ^{237}Np , and 10.0% for ^{27}Al and ^{58}Ni . Thus, the C/M benchmark comparison for the PCA indicates that the FANP calculations are exceptionally accurate, with no bias and a small standard deviation of [] The FANP calculations may be used for any LWR or other configurations of steel and water internal and vessel structures with an expected standard deviation []

G.4.2.2 NUREG/CR-6115 BWR Benchmark

Even though the PCA “blind test” was supposed to resolve the problem that the NRC had with inaccurate calculations of fluence rates throughout the industry, only Framatome ANP had results that were accurate enough to have valid calculations of vessel fluence values. Therefore, the other fluence analysts throughout the industry continued to “unfold” “measured” fluence values even though there were no vessel measurements. As part of Regulatory Guide 1.190, “Calculational And Dosimetry Methods For Determining Pressure Vessel Neutron Fluence,”^{G4} the NRC ended the concept of “unfolding” “measured” vessel fluence values. The regulatory guide required that vessel fluence predictions be based only on calculated results. Moreover, it was suggested that calculational benchmarks be performed for PWRs and a BWR. The benchmark calculations are described in NUREG/CR-6115 (6115).^{G5} The following summarizes the comparison of the FANP calculated results to the Brookhaven National Laboratory (BNL) results.

PROPRIETARY

The key to making a $FANP/BNL-6115$ comparison is the criteria developed to determine acceptable versus unacceptable deviations. Since both FANP and BNL analyzed the PCA, the criteria for acceptable deviations were developed from the PCA results. In view of the fact that the FANP calculations were the most accurate and the FANP database includes the PCA results, the FANP uncertainties were extracted from Revision 1 of this topical. The FANP calculations have no statistically significant bias and a standard deviation of [] The BNL results for the PCA were compared to the measurements and those from the FANP calculations. From this comparison, it was estimated that the BNL results in 6115 had no statistically significant bias and the standard deviation is on the order of the mean experimental uncertainty for the dosimetry 10.7%. Statistically combining these standard deviations indicates that the standard deviation of the FANP and 6115 comparison ($\overline{\sigma_{FANP/6115}}$) should be about [] However, considering that most of the modeling deviations associated with the neutron source, geometry, material composition, and modeling methods have been eliminated, the actual mean deviation should be statistically insignificant. Since an insignificant deviation is defined as one-third of the standard deviation, the FANP and 6115 comparison should agree to within []

The following figures depict the comparison of the FANP calculations and the 6115 results. The format of the figures follows that used in NUREG/CR-6115. The deviations are presented as a function of the azimuthal direction for a fixed radius and the axial location of the maximum fluence rate (306.605 centimeters).^{G5} The table below summarizes the key deviations from the figures.

PROPRIETARY

FANP/
BNL - 6115 **Comparison of Key Deviations**

[

| | | | |
|--|--|--|--|
| | | | |
| | | | |
| | | | |
| | | | |
| | | | |
| | | | |
| | | | |

Figure G-3

Figure G-4

Figure G-5

Figure G-6

Figure G-7

Figure G-8

]

The mean value of the first moment of the deviations is the “Mean Deviation” in the table above summarizing the key deviations from the figures. In each of the six radial locations, from the downcomer to the outside surface of the vessel, the mean deviation is less than [] Thus, as discussed above, the deviations between the FANP calculations and the 6115 results are insignificant.

While the combined standard deviation of the $FANP/6115$ comparison would be expected to be [], the standard deviation in each of the six radial locations is much less, varying from [

] Thus, it would appear that FANP calculations of BWRs are indeed accurate with a small mean random uncertainty.

Reviewing the figures, and the table of [

] Along the radial location of the downcomer, the standard deviation is [

] Likewise, along the vessel inside surface, the standard deviation is [] While random deviations of [

] Again, to model the cylindrical jet pump structures located at the various locations, [

] Therefore, the $FANP/_{6115}$ comparison indicates that the FANP calculational methodology is equally accurate for LWRs and other reactors with similar core neutronic characteristics and steel – water configurations in the internal and vessel structures.

While there is nothing more that can be inferred about the accuracy and random uncertainty of the FANP calculations from the 6115 benchmark comparison, there is an interesting comparison associated with the capsule results. The capsule in the BWR benchmark was located around the three degree azimuthal position. Around this position, there is a local bias as seen in Figures G-3 and G-4, and the table showing the “ $FANP/_{BNL-6115}$ Comparison of Key Deviations.” Thus, when the FANP dosimeter reaction rate calculations are compared to the 6115 values, there is an overall bias of [] This bias is the mean value from the table below which shows the dosimetry reaction rate comparison.

FANP/BNL-6115 Dosimetry Reaction Rate Comparison

[

| | | | | | |
|--|--|--|--|--|--|
| | | | | | |
| | | | | | |
| | | | | | |
| | | | | | |
| | | | | | |
| | | | | | |
| | | | | | |
| | | | | | |

]

If the “*FANP/BNL-6115* Dosimetry Reaction Rate Comparison” table above were to be used to adjust the vessel inside surface fluence rate values, all vessel fluence values would be biased by [] Whereas, the table providing the “*FANP/BNL-6115* Comparison of Key Deviations” shows that the vessel fluence values are accurate with an insignificant bias. This substantiates the fact that “unfolding” the vessel fluence based on a limited set of dosimetry measurements can be invalid.

G.4.2.3 Browns Ferry Unit 2 Capsule Benchmark

The Tennessee Valley Authority (TVA) provided Framatome ANP with a contract to refuel Browns Ferry Units 2 and 3 with blended low enriched uranium (BLEU) fuel. BLEU fuel does not have the same neutronic characteristics as normal low enriched uranium fuel. Consequently, the issue of fluence rate differences between BLEU and normal low enriched uranium fuel needed to be addressed. TVA wanted to ensure that the existing pressure – temperature curves continued to be valid. Thus, FANP performed

an analysis of the flux in Browns Ferry Units 2 and 3 with BLEU fuel. The results were a comparison of the BLEU fuel flux compared to the normal low enriched uranium fuel flux.

To ensure a consistent evaluation between the FANP and the GE Nuclear Energy (GENE) fluence rate, a benchmark of the Browns Ferry Unit 2 30° Capsule was evaluated. In Reference G6, GENE discusses the capsule fluence evaluation. They note that the flux wire measurement for the Browns Ferry Unit 2 Capsule included iron, copper and nickel dosimeters. The capsule was removed at the end of Cycle 7 during the refueling outage, following the October first, 1994 shutdown. The result in terms of neutrons per square centimeter – second was:

$$\textit{Measured Flux} = 5.9 \times 10^8$$

G12

GENE reports that their calculated flux was 9.5×10^8 giving a calculated to measured ratio of:

$$C/M \text{ (GENE)} = \frac{9.5 \times 10^8}{5.9 \times 10^8} = 1.61$$

The FANP calculations of the greater than 1.0 MeV flux, at a 100% rated power level of 3293 mega-Watts thermal, produced a result of 6.6×10^8 . The C/M ratio is therefore:

| | |
|---|-----|
| $C/M \left(\begin{array}{l} \text{Browns Ferry Unit 2} \\ \text{30 - Degree Capsule} \end{array} \right) \text{(FANP)} = \frac{6.6 \times 10^8}{5.9 \times 10^8} = 1.12$ | G13 |
|---|-----|

This benchmark of the Browns Ferry Unit 2 Capsule indicates that the FANP calculations for BWRs are very accurate and within the random uncertainty of the FANP database.

G.4.2.4 Analytic Sensitivity

The analytic sensitivity evaluation performed previously for the neutron source and geometry may be extended to the BWR modeling-procedure uncertainties. The BWR extensions for (1) the transport of neutrons from the core through the internal structures associated with the jet pumps, (2) the integrated core leakage function from the fuel, and (3) the three dimensional synthesis of the core flux function, represent a subset of the previous evaluations. The previous calculations have been updated and extended to treat the BWR modeling and procedures described in Sections G.3.2 through G.3.4. As noted with the previous analytical uncertainty evaluation, the results of the deviations have no

well-defined level of confidence. [

]

$$\sigma_c(\textit{Analytic}) = [\quad]$$

(G.14)

[]
a confidence factor of [] provides a 95% level of
confidence in the uncertainty with [] degrees of freedom.

[

]

$$\sigma_c(\textit{Dosimetry}) = [\quad]$$

(G.15)

G.4.3 Summary

Previous bias evaluations associated with the calculations are discussed in Section 7.2.1 of this topical. It is noted that not only are the measurements unbiased and highly accurate, but the mean value of the calculated neutron fluence values is also unbiased. The benchmark comparisons of the calculations to the dosimetry measurements indicate that there are no statistically significant biases associated with the fluence reactions with energies greater than 0.1 MeV. [

] the information presented above indicates that the BWR calculations have no statistically significant bias (B_C). This is represented by Equation G.16 below.

$$B_C(Fluence) = 0.0 \tag{G.16}$$

The BWR benchmarks discussed above indicate that the C/M comparisons are consistent with the FANP dosimetry database referenced in Appendix E. Thus, there is a 95% level of confidence that the mean BWR benchmark uncertainty ($\overline{\sigma_{C/M}}$) would not be greater than [] A confidence factor of [] degrees of freedom represents the calculational uncertainty, and a confidence factor of [] degrees of freedom represents

the measurement uncertainty. Equation G.17 gives the estimate of the BWR benchmark uncertainty []

$$\overline{\sigma_{C/M}} \text{ (BWR Dosimetry Benchmark) } = [] \quad (\text{G.17})$$

With [] degrees of freedom representing the calculational uncertainty, any one comparison of dosimetry calculations to measurements could have a mean random deviation in the C/M ratio of [

] such as the Browns Ferry Unit 2 benchmark which has a deviation of 12.0%.

Section 7.3 in this topical explains how the standard deviations from the analytic sensitivity evaluation were estimated to be consistent with [

] the vessel fluence standard deviation. Equation 7.22 forms part of the basis [

] and Equation 7.23 gives the combined standard deviation for the vessel. The uncertainty in Equation G.15 is sufficient to represent the fluence uncertainty at dosimetry locations. Utilizing Equations 7.22 and 7.23, the vessel fluence uncertainty is that shown by Equation G.18.

$$\sigma_C(BWR \text{ Vessel Fluence}) = [\quad] \quad (G.18)$$

The vessel fluence uncertainty, represented by the Equation G.18 standard deviation, is consistent with [] providing a 95% level of confidence that vessel fluence - embrittlement predictions will be within the uncertainty of the embrittlement database.

The Framatome ANP uncertainties associated with BWR dosimetry measurements and calculations are unbiased (Equation G.16) and have well-defined standard deviations for the appropriate levels of confidence. The extended models and procedures have an estimated dosimetry uncertainty from analytic sensitivity evaluations that is not greater than [] The combination [] gives a dosimetry standard deviation of []

The analytic sensitivity evaluation for the vessel uncertainty is not greater than [] Combining the analytic vessel standard deviation in a consistent manner [] indicates the vessel standard deviation is not greater than [] The uncertainty in the vessel fluence calculations needs to be less than 20.0% to be consistent with vessel embrittlement evaluations. Clearly, the vessel value of [] meets the criterion. Therefore, the Framatome ANP BWR fluence

methods and corresponding uncertainties are sufficient for BWR fluence - embrittlement analyses.

Appendix G References

- G1. Mark A. Rutherford, et al, "DORT, Two Dimensional Discrete Ordinates Transport Code, (BWNT Version of RISC/ORNL Code DORT)," FANP Document # BWNT-TM-107, May, 1995.
- G2. S. Sitaraman, et al, "Licensing Topical Report, General Electric Methodology for Reactor Pressure Vessel Fast Neutron Flux Evaluations," GE Nuclear Energy, Document # NEDO-32983-A, Revision 0, December, 2001.
- G3. Office of Nuclear Regulatory Research, "Calculational And Dosimetry Methods For Determining Pressure Vessel Neutron Fluence," U.S. Nuclear Regulatory Commission, Regulatory Guide 1.190, March, 2001.
- G4. W.N. McElroy "LWR Pressure Vessel Surveillance Dosimetry Improvement Program: PCA Experiments And Blind Test," Hanford Engineering Development Laboratory, NUREG/CR-1861 (HEDL-TME 80-87), July, 1981.
- G5. J.F. Carew, K. Hu, A. Aronson, A. Prince, G. Zamonsky, "PWR and BWR Pressure Vessel Fluence Calculation Benchmark Problems and Solutions," Brookhaven National Laboratory, NUREG/CR-6115 (BNL-NUREG-52395), September, 2001.
- G6. L.J. Tilly, B.D. Frew, B.J. Branlund, "Pressure – Temperature Curves for TVA Browns Ferry Unit 3," GE Nuclear Energy, GE-NE-0000-0013-3193-02a-R1, Revision 1, August, 2003.